Eur. Phys. J. B **26**, 375–378 (2002)
DOI: 10.1140/epjb/e20020102

THE EUROPEAN PHYSICAL JOURNAL B
EDP Sciences

Phonon heat transport in silicon nanowires

X. Lü[a] and J.H. Chu

National Laboratory for Infrared Physics, Shanghai Institute of Technical Physics, Chinese Academy of Science, Shanghai 200083, PR China

Received 24 April 2001 and Received in final form 23 December 2001

Abstract. Thermal conductivity of silicon and porous silicon nanowires based on the equation of phonon radiative transport is theoretically evaluated. The thermal conductivities of silicon nanowires with square cross-sections are found to match molecular dynamics simulation results reasonably well. It is shown that the results of meso-porous silicon nanowires are about two orders of magnitude lower than that of silicon nanowires in a wide range of temperature (50 K–300 K).

PACS. 63.20.Kr Phonon-electron and phonon-phonon interactions – 63.22.+m Phonons or vibrational states in low-dimensional structures and nanoscale materials – 65.40.-b Thermal properties of crystalline solids

1 Introduction

Transport in one- and two-dimensional structures has been the subject of intensive research. A number studies have carried on the conductivity of nanowires and quantum wires based on the Born approximation [1,2], steady-state Boltzmann's equations [3,4]. As a consequence of the rough boundaries scattering, the electrical conductivity values are reduced. However, the thermal behavior of nanowires with boundary scattering is little understood at this stage. Study of thermal phenomena in nanostructures requires to know the thermal conductivity of the material. Recently it is found that the thermal conductivity values of meso-porous silicon (meso-PS) are about two orders lower than corresponding data of bulk silicon (241 W/m K) [5–7]. It is explained that the size of nanocrystallities are smaller than the phonon mean free path (MFP) in bulk Si. So meso-PS is applied as new thermal insulating substrate for microsensor design. It is reported that the thermal conductivities of silicon (Si) nanowires has the similar properties based on molecular dynamics (MD) simulation [8]. The value is close to the thermal conductivity of SiO_2 (1.4 W/m K), which is known as good thermal insulators. So we can also apply the Si nanowires array to the domain of thermal sensors which require a thermal insulator. However, little effort has been made to study the size dependence of the thermal conductivity of nanowires. In this paper a study of the thermal conductivity in nanowires is reported here using the equations of phonon radiative transport (EPRT) method. We will explain the MD results of Si nanowires with the EPRT, assuming a partly diffuse-scattering interface. We also extend our model to calculate the thermal conductivity of meso-PS nanowires.

[a] e-mail: xianglu@mail.sitp.ac.cn

2 Equation of phonon radiative transport for a wire

The EPRT was derived from the Boltzmann transport equation (BTE) by phonons between two parallel plates. Omini *et al.* [9] presented the solution of phonon transport equation and thermal conductivity. Majumdar [10] recently developed the EPRT from the original BTE for thin films. Chen *et al.* established the EPRT on the in-plane and out-plane thermal conductivity of quantum wells [11], superlattices [12–14] based on the BTE. Volz *et al.* [15] calculated the thermal conductivity in clamped silicon nanowires with circular cross-sections on the basis of the EPRT. Now we extend the EPRT to thin square wires case. Let us consider a wire with square cross-section that has a side length a. The BTE of the wire can be written in the relaxation time approximation (RTA) as

$$v_z \frac{\partial f}{\partial T}\frac{\mathrm{d}T}{\mathrm{d}z} + v_x \frac{\partial f}{\partial x} + v_y \frac{\partial f}{\partial y} = -\frac{f - f_0}{\tau}\,. \qquad (1)$$

If wave vector $\boldsymbol{q}$ is chosen to have the linear form: $q = \omega/v$, the spectral phonon intensity, the flux of phonon energy per unit time, per unit area perpendicular to the direction of the phonon propagation, per unit solid angle in the direction of phonon propagation and per unit frequency interval around ω, can be expressed as

$$I_\omega(\boldsymbol{r}, \theta, \phi) = \frac{1}{4\pi} v_p(\theta, \phi) f_\omega(\boldsymbol{r}) \hbar\omega D(\omega). \qquad (2)$$

where $D(\omega)$ is the density of phonon states per unit volume, $f(\boldsymbol{r})$ the phonon distribution function, $v_p(\theta,\phi)$ the phonon group velocity in the direction of (θ,ϕ), θ and ϕ are the polar and azimuthal angles, respectively. $I_{\omega 0}$ is equilibrium phonon intensity. A solution of equation (1) can be obtained by introducing a deviation function i_ω:

$$I_\omega(\boldsymbol{r},\theta,\phi) = I_{\omega 0}(z) + i_\omega(\boldsymbol{r},\theta,\phi). \tag{3}$$

and neglecting its derivative in the z-direction. Equation (1) becomes

$$\sin\theta\cos\phi\frac{\partial i_\omega}{\partial x} + \sin\theta\sin\phi\frac{\partial i_\omega}{\partial y} + \frac{i_\omega}{\Lambda_\omega} = -\cos\theta\frac{\mathrm{d}I_{\omega 0}}{\mathrm{d}z}\cdot \tag{4}$$

where $\boldsymbol{r}$ is the coordinate directions vector, $\Lambda_\omega = \tau(T,\omega)v_p$ is the phonon mean free path (MFP).

The solution of the above equation can be obtained by the well established method in thermal radiation [16]

$$\begin{aligned} i_\omega^+(\gamma;\theta,\phi) = b^+(\theta,\phi)\Bigg\{&\Theta^+\exp\left(-\frac{\gamma}{\sin\theta\sin\phi}\right) \\ &+ (1-\Theta^+)\exp\left(-\frac{\gamma}{\sin\theta\cos\phi}\right)\Bigg\} \\ &- \cos\theta\Lambda_\omega\frac{\mathrm{d}I_{\omega 0}}{\mathrm{d}z}\Bigg\{\Theta^+\left[1-\exp\left(-\frac{\gamma}{\sin\theta\sin\phi}\right)\right] \\ &+ (1-\Theta^+)\left[1-\exp\left(-\frac{\gamma}{\sin\theta\cos\phi}\right)\right]\Bigg\} \\ &\left(0<\theta<\frac{\pi}{2}\right), \end{aligned} \tag{5}$$

$$\begin{aligned} i_\omega^-(\gamma;\theta,\phi) = b^-(\theta,\phi)\Bigg\{&\Theta^-\exp\left(\frac{\gamma_a-\gamma}{\sin\theta\sin\phi}\right) \\ &+ (1-\Theta^-)\exp\left(\frac{\gamma_a-\gamma}{\sin\theta\cos\phi}\right)\Bigg\} \\ &+ \cos\theta\Lambda_\omega\frac{\mathrm{d}I_{\omega 0}}{\mathrm{d}z}\Bigg\{\Theta^-\left[\exp\left(\frac{\gamma_a-\gamma}{\sin\theta\sin\phi}\right)-1\right] \\ &+ (1-\Theta^-)\left[\exp\left(\frac{\gamma_a-\gamma}{\sin\theta\cos\phi}\right)-1\right]\Bigg\} \\ &\left(\frac{\pi}{2}<\theta<\pi\right). \end{aligned} \tag{6}$$

where $\gamma(=x/\Lambda_\omega)$ is the dimensionless x coordinate, $\gamma_a(=a/\Lambda_\omega)$, is the dimensionless side length of the wire, respectively. Θ^+ and Θ^- are unit step functions. Θ^+=0 for $(x\tan\phi - y) < 0$ and Θ^+=1 for $(x\tan\phi - y) > 0$; Θ^-=0 for $[(a-x)\tan\phi - (b-y)] < 0$ and Θ^-=1 for $[(a-x)\tan\phi - (b-y)] > 0$. The local heat flux in the z direction can be obtained by integration over the solid angle as

$$\begin{aligned} q(\gamma) &= \int_{4\pi} I_\omega(\boldsymbol{r},\theta,\phi)\cos\theta\,\mathrm{d}\Omega \\ &= \frac{4}{a^2}\int_s \mathrm{d}s\int_0^{\omega_D}\mathrm{d}\omega\int_0^{2\pi}\mathrm{d}\phi\int_0^{\frac{\pi}{2}}[i_\omega^+(\gamma;\theta,\phi) \\ &\quad - i_\omega^-(\gamma;\theta,\phi)]\cos\theta\sin\theta\,\mathrm{d}\theta. \end{aligned} \tag{7}$$

Here $\mathrm{d}\Omega(=\int_0^{2\pi}\mathrm{d}\phi\sin\theta\,\mathrm{d}\theta)$ is the differential solid angle. The final expression for the heat flux depends on the interface conditions, which determine the coefficients $i_\omega^+(\gamma;\theta,\phi)$ and $i_\omega^-(\gamma;\theta,\phi)$ in equations (5, 6). Now we consider the limiting case where the interface scatters phonons purely diffusely. Substituting equations (5, 6) in equation (7) and performing the integration, we obtain the effective thermal conductivity perpendicular to the cross-section

$$\begin{aligned} \kappa(T,a) = &\frac{k_B}{2\pi^2 v}\left(\frac{k_B}{\hbar}\right)^3 T^3 \\ &\times\int_0^{\frac{\theta_D}{T}}\frac{\mu^4\mathrm{e}^\mu}{(\mathrm{e}^\mu-1)^2}\tau(T,\mu)g(\gamma_a(T,\mu))\,\mathrm{d}\mu, \end{aligned} \tag{8}$$

$$\begin{aligned} g(\gamma) = 1 - \frac{3}{4\gamma} + \frac{4}{5\pi\gamma^2} + \frac{6}{\pi\gamma}\int_0^{\frac{\pi}{4}}\Bigg[&(\cos\phi-\sin\phi) \\ &\times L_5\left(\frac{\gamma}{\cos\phi}\right) - \frac{1}{\gamma}\sin 2\phi L_6\left(\frac{\gamma}{\cos\phi}\right)\Bigg]\mathrm{d}\phi. \end{aligned} \tag{9}$$

where

$$L_n(u) = \int_0^{\frac{\pi}{2}}\exp\left(-\frac{u}{\sin\theta}\right)\cos^2\theta\sin^{n-3}\theta\,\mathrm{d}\theta. \tag{10}$$

where θ_D is the Debye temperature, v is the phonon group velocity, $\mu = \hbar\omega/kT$, $\gamma_a(T,\mu)$ is the ratio between the side length of the wire and phonon MFP, *i.e.*,

$$\gamma_a(T,\mu) = \frac{a}{\Lambda_\omega(T,\mu)}, \text{ with } \Lambda_\omega(T,\mu) = v\tau(T,\mu). \tag{11}$$

The results for partly diffuse scattering case can be obtained in terms of that for purely diffusing scattering

$$\kappa(T,a,\epsilon) = (1-\epsilon)^2\sum_{j=1}^{\infty} j\epsilon^{j-1}\kappa(T,ja) \tag{12}$$

where ϵ is the specular interface scattering fraction. The value of ϵ represents the probability that the carrier is undergoing a specular scattering event at the interface and takes on from 0 to 1. The value of 1-ϵ represents the probability that the carrier is undergoing a diffuse scattering event. The phonon relaxation time τ in the above equations can roughly be obtained based on the RTA. In RTA the relaxation time can be calculated by the summation of the inverse relaxation times for various scattering processes. In our model, we consider Umklapp process (U), isotope (or point) defect interaction (I), dislocation scattering (D), and boundary scattering (B) [17–19]. In order to take into account the different phonon scattering mechanisms, we used the following expression for the total phonon scattering rate τ^{-1}:

$$\begin{aligned} \tau^{-1} &= \left(\tau_U^{-1} + \tau_I^{-1} + \tau_D^{-1} + \tau_B^{-1}\right) \\ &= A\exp(-\theta_D/sT)T^3\omega^2 + B\omega^4 + C\omega + v/L \end{aligned} \tag{13}$$

where the four terms represent the scattering of phonons due to Umklapp process, at point defects, *via* dislocation

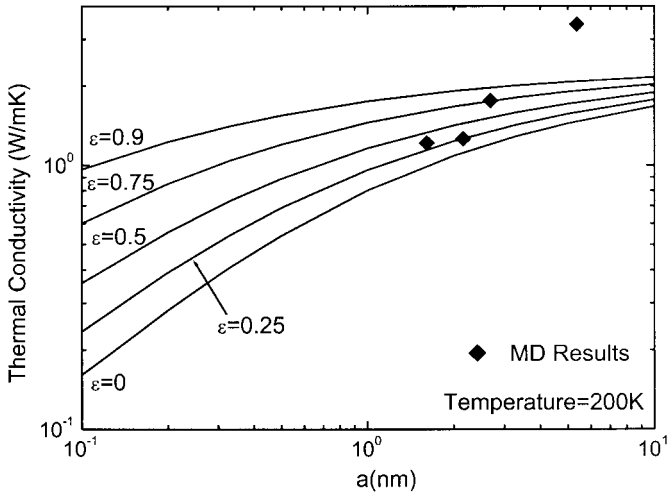

Fig. 1. Thermal conductivity as a function of side length of the nanowire at 200K. Data points from MD results and curves from the solution of the EPRT.

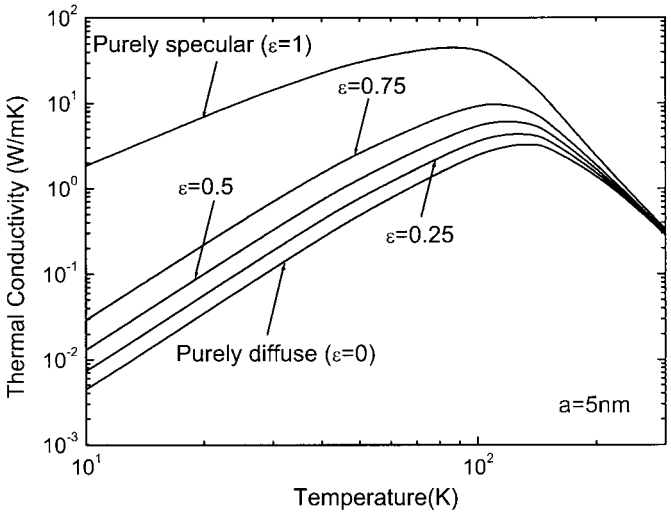

Fig. 2. Thermal conductivity as a function of temperature for different values of the interface scattering fraction ϵ according to the EPRT solution.

scattering, finally, *via* the scattering at sample boundaries, respectively. The parameter L is the characteristic length scale of sample. A, B, C, are materials constants. The parameter s for the Umklapp process is a constant characteristic of the vibrational spectrum of the materials.

3 Application to silicon and meso-porous silicon nanowires

Recently the thermal conductivity of Si nanowires is investigated using the MD simulations [8]. They use a solution of BTE to explain the possibility of explaining the MD results based on boundary scattering. Here, we will explore the MD results by solving the EPRT for thin square wires. The calculation for the thermal conductivity of Si nanowires is carried out based on equation (12). Since not all the scattering parameters are well known for Si nanowires, the interest was to obtain reasonable fitting values for all the parameters through direct comparisons between theory and the MD results. The overall set of parameters for calculation are given in Table 1 [20,21]. Numerical results of equation (12) are plotted as curves in Figures 1 and 2. The former shows the thermal conductivity as a function of the side length for the square cross-section. We note the EPRT and MD data are in good agreement when the specular interface scattering fraction ϵ value is about 0.25, which is quite different from the results of reference [8]. The reason is that we have calculated the thermal conductivity by the EPRT with an overall relaxation time $\tau(T,\mu)$, rather than the BTE with a constant relaxation time τ. This result reveals that our model is more reasonable than that of BTE, because τ is a function of frequency and temperature. Figure 2 shows the thermal conductivity as a function of the specular interface scattering fraction ϵ. One can see that the thermal conductivity is strongly temperature dependent and increases in the range of small temperatures and

Table 1. Parameters used for thermal conductivity calculation for Si nanowires at 200 K.

Parameter	Values
Crystal density (kg m^{-3})	2.33×10^{3}
Elastic constant (N m^{-2})	$c_{11}=16.67\times10^{10}$
	$c_{12}=6.45\times10^{10}$
	$c_{44}=7.99\times10^{10}$
Debye temperature (K)	650
Umklapp parameter A (s K^{-3})	8.5×10^{-21}
Isotope scattering parameter B (s^3)	2.4×10^{-44}
Dislocation scattering parameter C (s)	6.5×10^{-4}
Boundary scattering length L (m)	0.5×10^{-2}

has maximum value at $T \approx 100$ K. The side length of nanowires is $a = 5$ nm. For partially diffuse scattering our model predicts a lower value of thermal conductivity than that of purely specular scattering, *e.g.*, $\epsilon = 1$. It is found that thermal conductivity values are in the interval of 0.1–5 W/mK for $T > 100$ K, which is one to two orders of magnitudes smaller than that of monocrystalline Si (150 W/mK).

Finally we apply our model for a meso-PS nanowire and compare the results with those for Si nanowire. Lysenko *et al.* [6] reported a theoretical model describing thermal conductivity of meso-PS layers. Now we extend it to meso-PS nanowire with square cross-section, which combines our model for a Si nanowire (Eq. (12)) and Lysenko's model for a meso-PS layer. We find out the thermal conductivity $\kappa_{meso-PS}$ of the meso-PS nanowire can be written as

$$\kappa_{meso-PS} = \frac{k_B}{2\pi^2 v}\left(\frac{k_B}{\hbar}\right)^3 T^3(1-P)g_0 \int_0^{\frac{\theta_D}{T}} \frac{\mu^4 \mathrm{e}^{\mu}\tau(T,\mu)}{(\mathrm{e}^{\mu}-1)^2} \times \left[1+\frac{4}{3}\frac{\tau(T,\mu)}{r_{cr}}\right]^{-1} g(\gamma_a(T,\mu))\,\mathrm{d}\mu, \qquad (14)$$

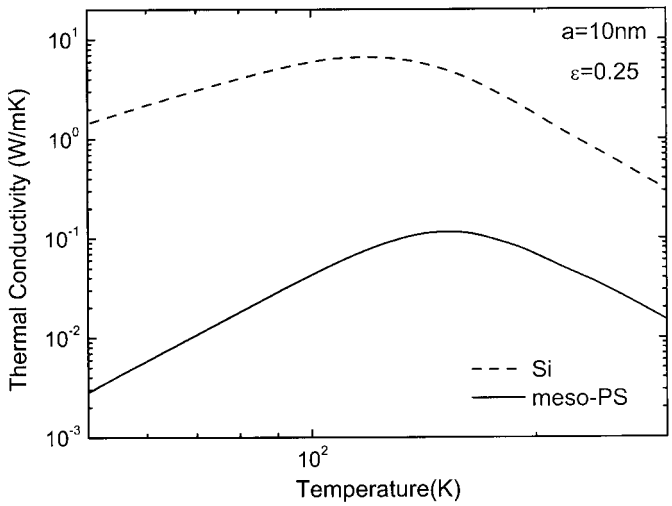

Fig. 3. Comparison the thermal conductivity of meso-PS nanowires and that of Si nanowires, as a function of the temperature.

where r_{cr} is the characteristic mean size of the nanocrystallite, P is the porosity, g_0 is the percolation strength. The fixed relation between g_0 and the porosity was given

$$g_0 = (1 - P)^2. \tag{15}$$

The temperature dependence of the thermal conductivity for a meso-PS nanowire of side length $a = 10$ nm and a Si nanowire of the same side length are shown in Figure 3. The characteristic mean size of the nanocrystallite is $r_{cr} = 7.2$ nm and the porosity is $P = 0.62$ [6]. One can see a larger reduction occurs in the meso-PS nanowire than that in the Si nanowire. The thermal conductivity of meso-PS nanowires is about two orders of magnitude lower than that of Si nannowires in a wide range of temperature (50 K–300 K). The porosity of meso-PS nanowires leads to the reduction of thermal conductivity. This result indicates that it is possible to decrease the thermal conductivity of meso-PS nanowires by increasing the porosity. The above discussed decreases in the thermal conductivity have been calculated for an isolated single nanowire. However, a microelectronic device always have a large number of wires parallel. So we can embed nanowire arrays in oriented meso-PS materials to obtain good thermal isolation. It can be applied for many types of thermal sensors.

4 Conclusion

The EPRT for thin wires with square cross-section developed from BTE is firstly applied in predicting the thermal conductivity of Si and meso-PS nanowires. Thermal conductivity in the direction of thickness is then obtained taking into account different scattering mechanisms under RTA. The calculation shows that side length and porosity for a nanowire have very strong effects on the thermal conductivity. With a specular interface scattering fraction value of 0.25, the numerical results of Si nanowires match the MD results reasonably well. It is found that the thermal conductivity of meso-PS nanowires are about two orders of magnitude smaller than that of Si nanowires. It is possible to decrease the thermal conductivity of the nanostructures by decreasing the side length and increasing the porosity. By synthesizing arrays of nanowires in meso-PS materials, we can obtain an excellent thermal isolation which can be applied for thermal sensors and thermal insulating substrate.

This work was supported by Natural Science Foundation of China and the special funds for Major State Basic Projet No. G001CB3095 of China.

References

1. G. Palasantzas, J. Barnaś, Phys. Stat. Sol. (b) **211**, 671 (1999).
2. G. Palasantzas, J. Barnaś, J.Th.M. De Hosson, J. Appl. Phys. **89**, 8002 (2001).
3. Y. Tokura, S. Tarucha, Phys. Rev. B **55**, 15 740 (1997).
4. H. Ruda, A. Shik, J. Appl. Phys. **86**, 5103 (1999).
5. V. Lysenko, V. Gliba, V. Strikha, A. Dittmsr, G. Delhomme, Ph. Roussel, D. Barbier, N. Jaffrezic-Renault, C. Martelet, Appl. Surf. Sci. **123**, 124 (1998).
6. V. Lysenko, S. Perichon, B. Remaki, D. Barbier, B. Champagnon, J. Appl. Phys. **86**, 6841 (1999).
7. V. Lysenko, S. Volz, Phys. Stat. Sol. (a) **182**, R6 (2000).
8. S.G. Volz, G. Chen, Appl. Phys. Lett. **75**, 2056 (1999).
9. M. Omini, A. Sparavigna, Phys. Rev. B **61**, 6677 (2000).
10. A. Majumdar, J. Heat Transf. **115**, 7 (1993).
11. G. Chen, C.L. Tien, J. Thermophys. Heat Transf. **7**, 311 (1993).
12. G. Chen, J. Heat Transf. **119**, 220 (1997).
13. G. Chen, Phys. Rev. B **57**, 14958 (1998).
14. G. Chen, M. Neagu, Appl. Phys. Lett. **71**, 2761 (1997).
15. S.G. Volz, D. Lemonnier, J.-B. Saulnier, Microscale Therm. Eng. **5**, 191 (2001).
16. R. Siegel, J. Howell, *Thermal Radiation Heat Transfer* (Hemisphere, Washington 1993).
17. J. Callaway, Phys. Rev. **113**, 1046 (1959).
18. P. Vonlanthen, S. Paschen, D. Pushin, A.D. Bianchi, H.R. Ott, J.L. Sarrao, Z. Fisk, Phys. Rev. B **62**, 3246 (2000).
19. R.P. Joshi, P.G. Neudeck, C. Fazi, J. Appl. Phys. **88**, 265 (2000).
20. H.H. Landholt, R. Börnstein, *Numerical Data and Functional Relationships in Science and Technology*, New Series, Vol. 1 (Springer, Berlin, 1966).
21. M. Newberger, S.J. Welles, *Silicon* (Hughes Aircraft Company, Culver City, CA, 1969), p. 1.